All Local Conserved Quantities of the One-Dimensional Hubbard Model

Kohei Fukai *

The Institute for Solid State Physics, The University of Tokyo, Kashiwa, Chiba 277-8581, Japan

(Received 16 January 2023; accepted 24 October 2023; published 22 December 2023)

We present the exact expression for all local conserved quantities of the one-dimensional Hubbard model. We identify the operator basis constructing the local charges and find that nontrivial coefficients appear in the higher-order charges. We derive the recursion equation for these coefficients, and some of them are explicitly given. There are no other local charges independent of those we obtained.

DOI: 10.1103/PhysRevLett.131.256704

Introduction.—Quantum integrability and local conservation laws are two sides of the same coin. Quantum integrable systems are exactly solvable many-body systems by the Bethe ansatz [1] and have an extensive number of local conserved quantities $\{Q_k\}_{k\geq 2}$, which is the foundation of their solvability. Recently, quantum integrable systems are becoming an arena for the studies of nonequilibrium quantum dynamics, inspired by their experimental realization with ultracold atoms [2–5], where Q_k play a crucial role: their existence leads to the absence of thermalization [6–8] and the conjectured longtime steady state is the generalized Gibbs ensemble [9–11], involving all local (and also quasilocal) conserved quantities as well as Hamiltonian [12–16]. The large-scale nonequilibrium behavior is described by generalized hydrodynamics [17,18], which is based on the local continuity equations of Q_k. In quantum inverse scattering methods [19,20], the existence of the local conserved quantities is understood from the commutativity of the transfer matrices $[T(\lambda), T(\mu)] = 0$: Q_k is obtained from the expansion of $\ln T(\lambda)$ in terms of the spectral parameter λ, and usually, the leading term $Q_2 = H$ is Hamiltonian itself. Another way to calculate Q_k is the use of the boost operator B [21–23] if it exists: local charges can be calculated recursively by $[B, Q_k] = Q_{k+1}$.

Although a procedure to generate the local conserved quantities Q_k has been known, it is still practically difficult to obtain their expressions. This difficulty lies not only in the expensive computational cost for higher-order charges but also in finding a general pattern in the huge amounts of data that emerge out of this calculation [24]. This problem has been investigated particularly for the spin-1/2 XYZ chain [25–32] and the one-dimensional Hubbard model [33–40]. The former case is now deeply understood: the explicit expressions for the isotropic XXX case are obtained independently in Refs. [41,42]. For the general XYZ case, Grabowski and Mathieu found the structure of Q_k and derived the recursion relations to construct Q_k using boost operator [24], and recently, its explicit expression was obtained by Nozawa and Fukai [43] using the doubling-product notation [44], and for the XXZ case, independently obtained by Nienhuis and Huijgen using the Temperley-Lieb algebra [45].

On the other hand, for the one-dimensional Hubbard model, the structure of the local conserved quantities Q_k remains a mystery. The problem is that there was no recursive way to construct them [46], unlike the XYZ case, because of the absence of the boost operator [24,48]. This comes from the fact that the Hubbard model is not Lorentz invariant due to the separation of spin and charge excitations with different velocities [49–51]. The first three nontrivial charges have been found before: Q_3 [35,38], Q_4 [52,53], and Q_5 [24]. From these expressions, Grabowski and Mathieu conjectured that Q_k is constructed of products of local conserved densities of spin-1/2 XX chain [24]. However, what kind of products of the XX charges are allowed in Q_k was unknown.

In this Letter, we reveal the structure of the local conserved quantities Q_k in the one-dimensional Hubbard model and present their exact expressions. We prove Q_k is a linear combination of *connected diagrams*, a notation for the particular kind of products of the XX charges. With this notation, we find the expressions of the higher-order charges $Q_{k\geq 6}$, and nontrivial coefficients appear there. We derive the recursion equation for these coefficients of the connected diagrams in Q_k. There are no other local charges independent of our Q_k, and any local charges are written in a linear combination of Q_k.

Hamiltonian and notations.—The Hamiltonian of the one-dimensional Hubbard model is

$$H = -2\sum_{j=1}^{L}\sum_{\sigma=\uparrow,\downarrow}\left(c_{j,\sigma}^{\dagger}c_{j+1,\sigma} + \text{H.c.}\right) + 4U\sum_{j=1}^{L}\left(n_{j,\uparrow} - \frac{1}{2}\right)\left(n_{j,\downarrow} - \frac{1}{2}\right), \tag{1}$$

where the periodic boundary condition is imposed and $n_{j\sigma} \equiv c_{j,\sigma}^{\dagger}c_{j,\sigma}$ and U is the coupling constant.

We denote the kth local conserved quantity in terms of the polynomial of U by

$$Q_k = \sum_{j=0}^{j_f} U^j Q_k^j, \tag{2}$$

where $j_f = k-1$ $(k-2)$ for even (odd) k and Q_k^j is independent of U. Q_k is a linear combination of operators that act on at most k adjacent sites. We determine Q_k^j to satisfy $[Q_k, H] = 0$.

We introduce some notations to represent Q_k. We define a *unit* of $+$ type starting from jth site by

$$\overbrace{\bigcirc\bigcirc\cdots\bigcirc}^{n}{}_{\sigma}(j) \coloneqq 2\left(c_{j,\sigma}c^{\dagger}_{j+n,\sigma} + (-1)^n c^{\dagger}_{j,\sigma}c_{j+n,\sigma}\right), \tag{3}$$

where $n(>0)$ is the *length* of the unit. We define the zero-length unit by $|_\sigma(j) \coloneqq 2n_{j,\sigma} - 1$, and define its type as $-$. A unit of $-$ type with nonzero length is defined by $\bigcirc\cdots\bigcirc|_\sigma(j)(= |\bigcirc\cdots\bigcirc_\sigma(j)) \coloneqq |_\sigma(j) \times \bigcirc\cdots\bigcirc_\sigma(j)$ [54].

A *diagram* represents a product of units, denoted by $\Psi(i) = \prod_{\alpha=1}^{l_\Psi} \psi_{\sigma_\alpha}^{t_\alpha,n_\alpha}(j_{\alpha,i})$, where $\psi_\sigma^{t,n}(j)$ is the unit starting from the jth site with type t, length n, and spin σ, and $j_{\alpha,i} \equiv i + j_\alpha$, $j_1 = 0$, $j_\alpha \le j_{\alpha+1}$. j_α and σ_α satisfy if $\sigma_\alpha = \sigma_\beta(\alpha < \beta)$, then $j'_\alpha < j_\beta$ $(j'_\alpha \equiv j_\alpha + n_\alpha)$ and if $j_\alpha = j_{\alpha+1}$, then $\sigma_\alpha = \uparrow$, $\sigma_{\alpha+1} = \downarrow$. l_Ψ is the number of units in $\Psi(i)$. Units in a diagram mutually commute. A diagram $\Psi(i)$ has a graphical representation by a two-row sequence: $\psi_{\sigma_\alpha}^{t_\alpha,n_\alpha}(j_{\alpha,i})$ is placed on the upper (lower) row for $\sigma_\alpha = \uparrow$ $(\downarrow)$, with j_α columns being on its left. Positions without a unit are filled with "I." For example, the diagram $\Psi(i) = \psi_\uparrow^{-,2}(i)\psi_\downarrow^{+,3}(i+1)\psi_\uparrow^{-,1}(i+4)$ is represented as

(4)

Note that units on the same row are separated by I's. The interaction term is written as $\Big|(j) = |_\uparrow(j) \times |_\downarrow(j)$. A diagram without a site index denotes the site translation summation, $\Psi \coloneqq \sum_{i=1}^{L} \Psi(i)$.

We define some integers for a diagram Ψ. First, we define p_i by $\{p_1, \ldots, p_{2l_\Psi}\} = \{j_1, \ldots, j_{l_\Psi}, j'_1, \ldots, j'_{l_\Psi}\}$ where $p_i \le p_{i+1}$. Then, we define *support* by $s_\Psi \coloneqq j_{l_\Psi} + n_{l_\Psi} + 1$, *double* by $d_\Psi \coloneqq \sum_{i=1}^{l_\Psi - 1}(p_{2i+1} - p_{2i})$, *gap number* by $g_\Psi \coloneqq \sum_{i=1}^{l_\Psi-1} \delta_i(p_{2i+1} - p_{2i})$, where $\delta_i = 1$ for $p_{2i+1} \in \{j_1, \ldots, j_{l_\Psi}\}$, and otherwise 0. $s_\Psi - 1$ corresponds to the total number of columns in the two-row graphical representation of Ψ. We refer to a column $\substack{\bigcirc \\ \bigcirc}$ $\left(\substack{\text{I} \\ \text{I}}\right)$ as *overlap* (*gap*). g_Ψ (d_Ψ) corresponds to the total number of columns of gap (gap and overlap). (s, d) diagram is a diagram satisfying $s_\Psi = s$ and $d_\Psi = d$. We note that $s_\Psi > d_\Psi \ge g_\Psi$. For the diagram of Eq. (4), the integers are $(s_\Psi, d_\Psi, g_\Psi, l_\Psi) = (6, 1, 0, 3)$.

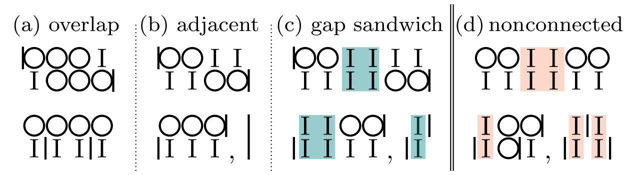

FIG. 1. Examples of connections of units (a)–(c), and the nonconnected diagrams (d). Units on the upper and lower rows of the diagrams in (a)–(c) are connected. The gaps in (c) [(d)] are indicated by the teal [orange] shaded area. The diagram on the bottom right in (d) does not satisfy condition (ii), while the others do not satisfy (i).

Two units in a diagram Ψ, indexed by α and $\beta(\alpha < \beta)$, are *connected* if $\sigma_\alpha \ne \sigma_\beta$ and for any $\gamma(\ne \alpha, \beta)$, either of $j'_\gamma < j'_\alpha$ or $j_\beta < j_\gamma$ holds. This condition can be categorized into three cases, as illustrated in Figs. 1(a)–1(c). A *connected diagram* is a diagram satisfying (i) for any two units in a diagram, indexed by α and β, there exists a sequence of indices of unit $(\alpha = \gamma_0, \gamma_1, \ldots, \gamma_N, \gamma_{N+1} = \beta)$, where the γ_ith and γ_{i+1}th units are connected, and (ii) the type of αth unit is $t_\alpha = (-)^{C_\alpha}$, where C_α is the number of units connected with it. The diagrams in Figs. 1(a)–1(c) and Eq. (4) are connected diagrams, and examples of nonconnected diagrams are given in Fig. 1(d). We found that Q_k is a linear combination of connected diagrams.

Structure of Q_k.—We show the explicit form of lower-order charges previously found in terms of connected diagrams: $Q_2 = H = \substack{\bigcirc \\ \text{I}} + \substack{\text{I} \\ \bigcirc} + U\Big|$ and $Q_3 = \substack{\bigcirc\bigcirc \\ \text{I}\ \text{I}} + U\left(\substack{\bigcirc| \\ \text{I}|} + \substack{|\bigcirc \\ |\text{I}}\right) + \updownarrow$, where $\updownarrow$ represents the diagrams with the upper and lower rows reversed, excluding those that remain invariant under this operation. Q_4 and Q_5 are written as

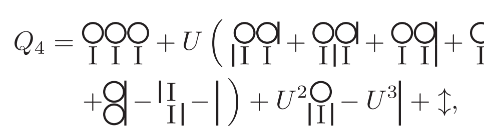

(5)

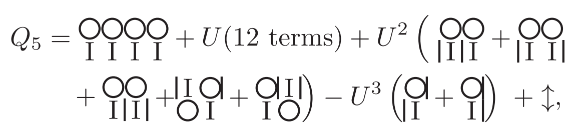

(6)

where we omit the 12 terms of Q_5^1. We newly obtained the explicit forms of higher-order Q_k for $k \ge 6$ and found nontrivial coefficients that are not ± 1 appear; for example,

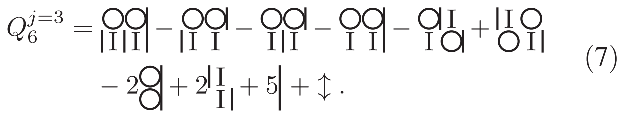

We give the explicit forms of Q_6, Q_7, Q_8 as examples of higher-order Q_k in Ref. [55].

The diagrams in Q_k^j are classified as (s,d)-connected diagrams as shown in Figs. 2 and 3, where circles represent (s,d)-connected diagrams in Q_k^j, and crosses represent diagrams generated by the commutator with the Hamiltonian $H = H_0 + UH_1$, where $H_0 =$ + ↕ and $H_1 =$ |. The solid arrow in Figs. 2 and 3 indicates the commutator with H_0. The vertical dotted arrow in Fig. 3 indicates the commutator with H_1. The diagrams at the crosses are to be canceled for the conservation law.

We give an example of commutators of units with H_0 and H_1 [56]: $[\ \cdot\ , H_0] = \ldots$ and $[\ \cdot\ , H_1] = \ldots$. The commutator of connected diagrams and H also generates a nonconnected diagram; the details are given in Ref. [55]. We can construct Q_k^j recursively by calculating the cancellation at the crosses in Fig. 3 from top to bottom.

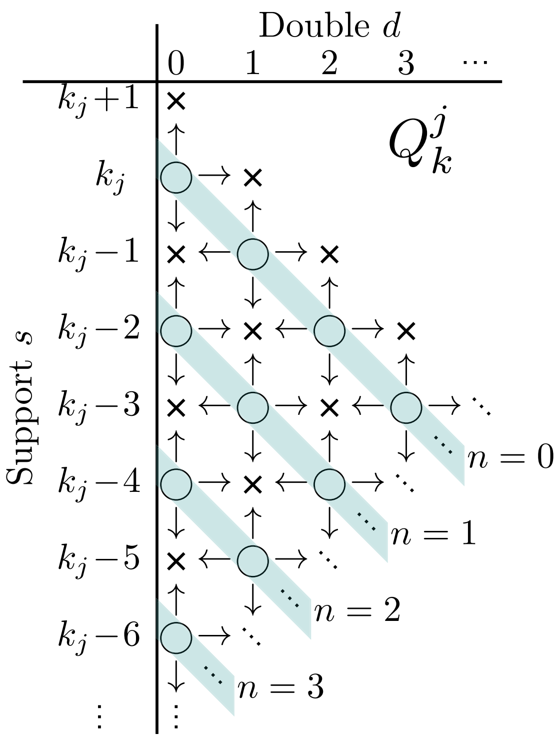

FIG. 2. Structure of Q_k^j. $k_j \equiv k - j$. Circles at (s,d) represent (s,d)-connected diagrams in Q_k^j $(s > d)$. The commutator of diagrams in the circle at (s,d) with H_0 generates the diagrams in the crosses at $(s \pm 1, d)$ and $(s, d \pm 1)$, indicated by the solid arrow tip.

Exact expressions.—We define *list* of diagram Ψ, $\boldsymbol{\lambda}_\Psi = \{\lambda_1, \lambda_2, \ldots, \lambda_{l_\Psi}\}$ by $\lambda_\alpha = p_{2\alpha} - p_{2\alpha-1} - \eta_\alpha$, where $\eta_\alpha = 0$ for $\alpha \in \{1, l_\Psi\}$ and otherwise $\eta_\alpha = 1$. λ_i represents the length of a sequence of *coast*, which we define as consecutive columns of ⋯ ⋯ or ⋯ ⋯, as illustrated:

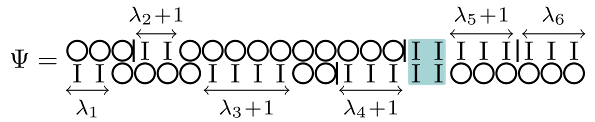

where $\boldsymbol{\lambda}_\Psi = \{2, 1, 3, 2, 2, 3\}$, and Ψ is the (24,6)-connected diagram and $g_\Psi = 2$ and $l_\Psi = 6$. The lengths of the coasts are indicated by the arrows, and the gap is indicated by the shaded area.

We show the exact expression of Q_k. Q_k^0 is the $(k,0)$ diagram: $Q_k^0 = \overbrace{\cdots}^{k-1} +$ ↕. Note that Q_k^0 is the local charge for the $U = 0$ case. For $Q_k^j (j \geq 1)$, we obtain the following result.

Theorem 1.—For $j \geq 1$,

$$Q_k^j = \sum_{\substack{0 \leq n+d < \lceil \frac{k-j}{2} \rceil, \\ n,d \geq 0}} \sum_{m=0}^{\lfloor \frac{j-1}{2} \rfloor} \sum_{g=0}^{d} (-1)^{n+m+g} \sum_{\Psi \in \mathcal{S}_{n,d,g}^{k,j,m}} C_{n,d}^{j,m}(\boldsymbol{\lambda}_\Psi)\Psi, \quad (8)$$

where $\mathcal{S}_{n,d,g}^{k,j,m}$ is the set of $(k-j-2n-d, d)$-connected diagrams Ψ with $l_\Psi = j+1-2m$ and $g_\Psi = g$. $C_{n,d}^{j,m}(\lambda_1 \ldots \lambda_l) \in \mathbb{Z}_{>0}$ is invariant under the permutation of $\lambda_i (2 \leq i \leq l-1)$, and the exchange of λ_1 and λ_l.

We note that the freedom to add $Q_{k'<k}$ to Q_k is fixed by the above choice of Q_k^0 and the constraint of $l_\Psi \geq 2$ for the diagram Ψ in $Q_k^j (j \geq 1)$. In this normalization, $Q_{2k}(Q_{2k+1})$ is even (odd) under mirror reflection. Our normalization is different from some of the previous studies. For example, the fourth charge of Ref. [24] is $Q_4 + U^2 H$ in the spin variable notation [54]. (s,d)-connected diagrams in Q_k^j have the same coefficients if the lists are identical up to the permutation explained above. $C_{n,d}^{j,m}(\boldsymbol{\lambda}_\Psi)$ satisfies some other nontrivial identities given in Ref. [55].

Theorem 2.—$C_{n,d}^{j,m}(\boldsymbol{\lambda})$ is calculated from the following recursion equation:

$$C_{n,d}^{j,m}(\boldsymbol{\lambda}) = C_{n,d}^{j,m}(\mathcal{T}\boldsymbol{\lambda}) + \sum_{\tilde{n}=0}^{n} (n+1-\tilde{n}) \times \left(C_{\tilde{n},n+d-\tilde{n}}^{j-1,m-1}(\boldsymbol{\lambda}_{\leftarrow 0}) - C_{\tilde{n},n+d-\tilde{n}}^{j-1,m-1}({}_{0\to}\mathcal{T}\boldsymbol{\lambda}) \right), \quad (9)$$

where $\mathcal{T}\boldsymbol{\lambda} = \{\lambda_1 - 1, \lambda_2, \ldots, \lambda_{l-1}, \lambda_l + 1\}$, ${}_{0\to}\boldsymbol{\lambda} = \{0, \lambda_1, \ldots\}$, $\boldsymbol{\lambda}_{\leftarrow 0} = \{\ldots, \lambda_l, 0\}$, and $l \equiv j + 1 - 2m$. For $\lambda_1 = -1$

case, we define $C^{j,m}_{n,d}(-1,\lambda_2,\ldots)\equiv C^{j,m}_{n,d-1}(1,\lambda_2,\ldots)$ for $d>0$ and $C^{j,m}_{n,d=0}(-1,\lambda_2,\ldots)\equiv C^{j,m}_{n-1,1}(0,\lambda_2-1,\ldots)+C^{j-1,m}_{n,0}(\lambda_2+1,\ldots)$. The initial condition is $C^{j=1,m=0}_{n,d}(\boldsymbol{\lambda})=1$. $C^{j,m}_{n,d}(\boldsymbol{\lambda})=0$ if $\lambda_i<0$ $(1<i<l)$ or $n<0$ or $m<0$ or $m\geq\lfloor j/2\rfloor$.

We obtained the general expressions of $C^{j,m}_{n,d}(\boldsymbol{\lambda})$ for some cases. For $n=0$ and $m=0$ case, we have

$$C^{j,m}_{n=0,d}(\boldsymbol{\lambda})=\binom{j-1+d}{m}-\binom{j-1+d}{m-1}, \tag{10}$$

$$C^{j,m=0}_{n,d}(\boldsymbol{\lambda})=\sum_{x_2=0}^{\lambda_2}\cdots\sum_{x_j=0}^{\lambda_j}\theta\left(n-\sum_{i=2}^{j}x_i\right), \tag{11}$$

where $j>1$ and $\theta(x)=1$ for $x\geq0$ and $\theta(x)=0$ for $x<0$. $C^{j,m}_{n=0,d}(\boldsymbol{\lambda})$ is independent of $\boldsymbol{\lambda}$ and $C^{j,m=0}_{n,d}(\boldsymbol{\lambda})$ is independent of $\lambda_1,\lambda_{j+1},d$. We note that Eq. (10) is the generalized Catalan number [24,42,57]. The expressions are more complicated for the n, $m>0$ case. For $j=3$, $m=1$ case, we have

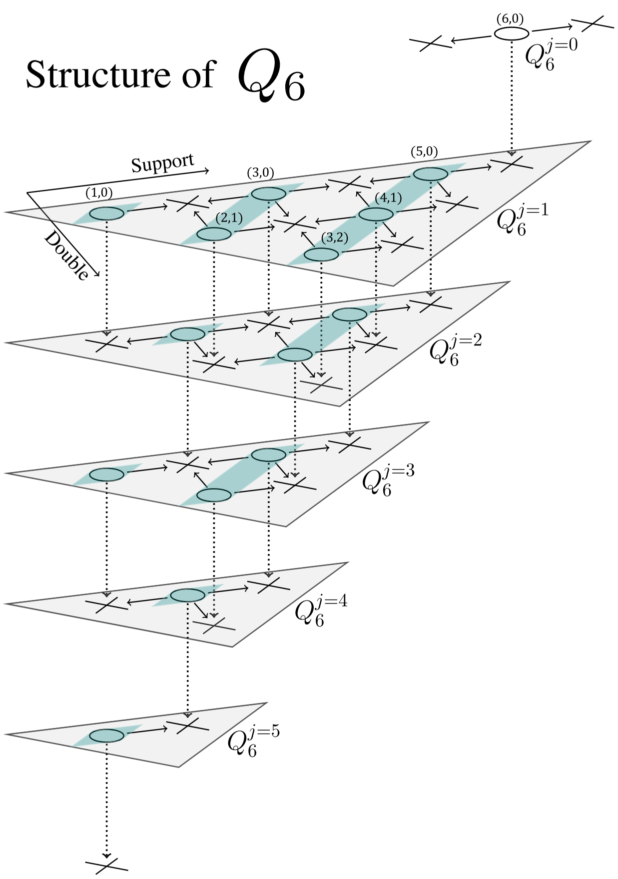

FIG. 3. Structure of Q_k for $k=6$. Each plane represents the structure of Q^j_k in Fig. 2. The commutator of diagrams in the circle at (s,d) in Q^{j-1}_k with H_{int} generates diagrams in the cross at (s,d) in Q^j_k, indicated by the vertical dotted arrow tip. The diagrams generated in the crosses are to be canceled.

$$C^{j=3,m=1}_{n,d}(\lambda_1,\lambda_2)=\sum_{\eta=\lambda_1,\lambda_2}\sum_{x=1}^{\eta}\binom{n+3-x}{3}+2\binom{n+4}{4}+(d-1)\left\{2\binom{n+3}{3}-\binom{n+2}{2}\right\}. \tag{12}$$

We also obtained the explicit expression of Q^2_k, Q^3_k for all k from Eqs. (11) and (12).

Through the Jordan-Wigner transformation [24], the 1D Hubbard model is mapped to a spin system, resulting in coupled XX chains, and a unit becomes the local conserved density in the XX chain: $\psi^{\pm,n(>0)}_{\mu}(i)\propto\sigma^x_{i,\mu}\sigma^z_{i+1,\mu}\cdots\sigma^z_{i+n-1,\mu}\sigma^{\bar{x}}_{i+n,\mu}+s\times(x\leftrightarrow y)$ and $\psi^{-,0}_{\mu}(i)=\sigma^z_{i,\mu}$, where $\sigma^{\alpha}_{i,\mu}$ is the Pauli matrix of flavor μ, and $s=\mp(-1)^n$ and $\bar{x}=x(y)$ for $s=1(-1)$ [54].

There are no other local conserved quantities independent of Q_k [58]. This is shown as follows: if F_k is a k-support charge, we can prove F_k is written as $F_k=c_kQ_k+F_{k-1}$, where F_{k-1} is a less than $(k-1)$-support charge and $c_k(\neq0)$ is some coefficient. Repeating this argument to F_{k-1} and so on, we can see F_k is a linear combination of $\{Q_l\}_{l\leq k}$. The details of this proof are given in Ref. [58].

From this completeness of our charges, we can see our Q_k is written as a linear combination of local charges obtained from the transfer matrix, and we can confirm the mutual commutativity of our charges, $[Q_k,Q_l]=0$, and their SO(4) symmetry [47]. Our Q_k coincides with the transfer matrix charges [53] at least up to Q_4.

Summary and outlook.—We presented the exact expression for the local charges of the 1D Hubbard model Q_k. In Theorem 1, we proved Q_k is constructed of the connected diagram, which represents the product of units, conserved densities of the XX chain in the spin variable notation, satisfying the conditions (i) and (ii). The diagrams constructing Q_k are accompanied by nontrivial coefficients [55] for $k\geq6$. These coefficients can be calculated by the recursion equation in Theorem 2. Some of them are the generalized Catalan numbers (10), which are also appearing in the local charges of the Heisenberg chain [24,41,42,57]. Deriving the general explicit formula for the coefficients is the remaining task, which may be some further generalization of the Catalan number. Our result is valid in both finite systems and the thermodynamic limit.

Our results have several applications: we can study the generalized Gibbs ensemble [12], current mean value formula and the generalized hydrodynamics [59–62], and factorization of correlation functions using local charges [63] in the 1D Hubbard model. A model with fragmented Hilbert space can be derived by considering the strong coupling limit of the local charges in the XXZ chain [64]. It is interesting to see what would happen in our case. Recently, it has been shown that the quantum many-body scarring model can be constructed using odd-order charges Q_{2k+1} [65]. We may make an immediate application of our result also for this direction.

To our knowledge, this is the first time revealing the structure of local conserved quantities in an integrable system without the boost operator, i.e., without a recursive way to construct them.

The work was supported by Forefront Physics and Mathematics Program to Drive Transformation (FoPM), WINGS Program, JSR Fellowship, the University of Tokyo, and KAKENHI Grant No. JP21J20321 from the Japan Society for the Promotion of Science (JSPS).

*k.fukai@issp.u-tokyo.ac.jp

[1] H. Bethe, Zur Theorie der Metalle, Z. Phys. **71**, 205 (1931).
[2] T. Kinoshita, T. Wenger, and D. S. Weiss, A quantum Newton's cradle, Nature (London) **440**, 900 (2006).
[3] I. Bloch, J. Dalibard, and W. Zwerger, Many-body physics with ultracold gases, Rev. Mod. Phys. **80**, 885 (2008).
[4] A. Polkovnikov, K. Sengupta, A. Silva, and M. Vengalattore, Colloquium: Nonequilibrium dynamics of closed interacting quantum systems, Rev. Mod. Phys. **83**, 863 (2011).
[5] T. Langen, T. Gasenzer, and J. Schmiedmayer, Prethermalization and universal dynamics in near-integrable quantum systems, J. Stat. Mech. (2016) 064009.
[6] A. C. Cassidy, C. W. Clark, and M. Rigol, Generalized thermalization in an integrable lattice system, Phys. Rev. Lett. **106**, 140405 (2011).
[7] M. Mierzejewski and L. Vidmar, Quantitative Impact of Integrals of motion on the eigenstate thermalization hypothesis, Phys. Rev. Lett. **124**, 040603 (2020).
[8] K. Fukai, Y. Nozawa, K. Kawahara, and T. N. Ikeda, Noncommutative generalized Gibbs ensemble in isolated integrable quantum systems, Phys. Rev. Res. **2**, 033403 (2020).
[9] M. Rigol, V. Dunjko, V. Yurovsky, and M. Olshanii, Relaxation in a completely integrable many-body quantum system: An *ab initio* study of the dynamics of the highly excited states of 1D lattice hard-core bosons, Phys. Rev. Lett. **98**, 050405 (2007).
[10] T. Langen, S. Erne, R. Geiger, B. Rauer, T. Schweigler, M. Kuhnert, W. Rohringer, I. E. Mazets, T. Gasenzer, and J. Schmiedmayer, Experimental observation of a generalized Gibbs ensemble, Science **348**, 207 (2015).
[11] L. Vidmar and M. Rigol, Generalized Gibbs ensemble in integrable lattice models, J. Stat. Mech. (2016) 064007.
[12] B. Pozsgay, The generalized Gibbs ensemble for Heisenberg spin chains, J. Stat. Mech. (2013) P07003.
[13] B. Wouters, J. De Nardis, M. Brockmann, D. Fioretto, M. Rigol, and J.-S. Caux, Quenching the anisotropic Heisenberg chain: Exact solution and generalized Gibbs ensemble predictions, Phys. Rev. Lett. **113**, 117202 (2014).
[14] B. Pozsgay, M. Mestyán, M. A. Werner, M. Kormos, G. Zaránd, and G. Takács, Correlations after quantum quenches in the *XXZ* spin chain: Failure of the generalized Gibbs ensemble, Phys. Rev. Lett. **113**, 117203 (2014).
[15] E. Ilievski, M. Medenjak, and T. Prosen, Quasilocal conserved operators in the isotropic Heisenberg spin-$1/2$ chain, Phys. Rev. Lett. **115**, 120601 (2015).
[16] E. Ilievski, J. De Nardis, B. Wouters, J.-S. Caux, F. H. L. Essler, and T. Prosen, Complete generalized Gibbs ensembles in an interacting theory, Phys. Rev. Lett. **115**, 157201 (2015).
[17] O. A. Castro-Alvaredo, B. Doyon, and T. Yoshimura, Emergent hydrodynamics in integrable quantum systems out of equilibrium, Phys. Rev. X **6**, 041065 (2016).
[18] B. Bertini, M. Collura, J. De Nardis, and M. Fagotti, Transport in out-of-equilibrium *XXZ* chains: Exact profiles of charges and currents, Phys. Rev. Lett. **117**, 207201 (2016).
[19] V. E. Korepin, N. M. Bogoliubov, and A. G. Izergin, *Quantum Inverse Scattering Method and Correlation Functions*, Cambridge Monographs on Mathematical Physics (Cambridge University Press, Cambridge, England, 1993).
[20] R. J. Baxter, *Exactly Solved Models in Statistical Mechanics* (Academic, New York, 1982).
[21] M. G. Tetel'man, Lorentz group for two-dimensional integrable lattice systems, Sov. Phys. JETP **55**, 306 (1982).
[22] K. Sogo and M. Wadati, Boost operator and its application to quantum Gelfand-Levitan equation for Heisenberg-Ising chain with spin one-half, Prog. Theor. Phys. **69**, 431 (1983).
[23] H. B. Thacker, Corner transfer matrices and Lorentz invariance on a lattice, Physica (Amsterdam) **18D**, 348 (1986).
[24] M. P. Grabowski and P. Mathieu, Structure of the conservation laws in quantum integrable spin chains with short range interactions, Ann. Phys. (N.Y.) **243**, 299 (1995).
[25] B. Sutherland, Two-dimensional hydrogen bonded crystals without the ice rule, J. Math. Phys. (N.Y.) **11**, 3183 (1970).
[26] R. J. Baxter, Eight-vertex model in lattice statistics, Phys. Rev. Lett. **26**, 832 (1971).
[27] R. J. Baxter, One-dimensional anisotropic Heisenberg chain, Phys. Rev. Lett. **26**, 834 (1971).
[28] R. J. Baxter, Partition function of the eight-vertex lattice model, Ann. Phys. (N.Y.) **70**, 193 (1972).
[29] R. J. Baxter, One-dimensional anisotropic Heisenberg chain, Ann. Phys. (N.Y.) **70**, 323 (1972).
[30] R. Baxter, Eight-vertex model in lattice statistics and one-dimensional anisotropic Heisenberg chain. I. Some fundamental eigenvectors, Ann. Phys. (N.Y.) **76**, 1 (1973).
[31] R. Baxter, Eight-vertex model in lattice statistics and one-dimensional anisotropic Heisenberg chain. II. Equivalence to a generalized ice-type lattice model, Ann. Phys. (N.Y.) **76**, 25 (1973).
[32] R. Baxter, Eight-vertex model in lattice statistics and one-dimensional anisotropic Heisenberg chain. III. Eigenvectors of the transfer matrix and Hamiltonian, Ann. Phys. (N.Y.) **76**, 48 (1973).
[33] E. H. Lieb and F. Y. Wu, Absence of Mott transition in an exact solution of the short-range, one-band model in one dimension, Phys. Rev. Lett. **20**, 1445 (1968).
[34] B. S. Shastry, Infinite conservation laws in the one-dimensional Hubbard model, Phys. Rev. Lett. **56**, 1529 (1986).

[35] B. S. Shastry, Exact integrability of the one-dimensional Hubbard model, Phys. Rev. Lett. **56**, 2453 (1986).
[36] E. Olmedilla, M. Wadati, and Y. Akutsu, Yang-Baxter relations for spin models and fermion models, J. Phys. Soc. Jpn. **56**, 2298 (1987).
[37] E. Olmedilla and M. Wadati, Conserved quantities of the one-dimensional Hubbard model, Phys. Rev. Lett. **60**, 1595 (1988).
[38] B. Sriram Shastry, Decorated star-triangle relations and exact integrability of the one-dimensional Hubbard model, J. Stat. Phys. **50**, 57 (1988).
[39] M. J. Martins and P. B. Ramos, The quantum inverse scattering method for Hubbard-like models, Nucl. Phys. **B522**, 413 (1998).
[40] F. H. L. Essler, H. Frahm, F. Göhmann, A. Klümper, and V. E. Korepin, *The One-Dimensional Hubbard Model* (Cambridge University Press, Cambridge, England, 2005).
[41] V. V. Anshelevich, First integrals and stationary states for quantum Heisenberg spin dynamics, Theor. Math. Phys. **43**, 107 (1980).
[42] M. P. Grabowski and P. Mathieu, Quantum integrals of motion for the Heisenberg spin chain, Mod. Phys. Lett. A **09**, 2197 (1994).
[43] Y. Nozawa and K. Fukai, Explicit construction of local conserved quantities in the XYZ spin-$1/2$ chain, Phys. Rev. Lett. **125**, 090602 (2020).
[44] N. Shiraishi, Proof of the absence of local conserved quantities in the XYZ chain with a magnetic field, Europhys. Lett. **128**, 17002 (2019).
[45] B. Nienhuis and O. E. Huijgen, The local conserved quantities of the closed XXZ chain, J. Phys. A **54**, 304001 (2021).
[46] Though the conserved quantities for the Hubbard model are studied by the expansion of the transfer matrix [37], it is not an easy task to obtain our local Q_k from the expansion transfer matrix, as noted in Ref. [47].
[47] M. Shiroishi, H. Ujino, and M. Wadati, SO(4) symmetry of the transfer matrix for the one-dimensional Hubbard model, J. Phys. A **31**, 2341 (1998).
[48] Though the generalization of boost operator for the Hubbard model was studied in Ref. [49], it seems difficult to obtain our Q_k using it because it has a differential operator and needs qualitatively different treatment from the usual boost operator, as noted in Ref. [50].
[49] J. Links, H. Q. Zhou, R. H. McKenzie, and M. D. Gould, Ladder operator for the one-dimensional Hubbard model, Phys. Rev. Lett. **86**, 5096 (2001).
[50] T. Yoshimura and H. Spohn, Collision rate ansatz for quantum integrable systems, SciPost Phys. **9**, 40 (2020).
[51] H. Frahm and V. E. Korepin, Critical exponents for the one-dimensional Hubbard model, Phys. Rev. B **42**, 10553 (1990).
[52] H. Grosse, The symmetry of the Hubbard model, Lett. Math. Phys. **18**, 151 (1989).
[53] H. Q. Zhou, L. J. Jiang, and J. G. Tang, Some remarks on the Lax pairs for a one-dimensional small-polaron model and the one-dimensional Hubbard model, J. Phys. A **23**, 213 (1990).
[54] Via Jordan-Wigner transformation [24], units are mapped to the spin variable notation, and they can be efficiently expressed by the doubling product [44].
[55] See Supplemental Material at http://link.aps.org/supplemental/10.1103/PhysRevLett.131.256704 for the proof of Theorems 1 and 2 and identities of the coefficients and the commutation relation of diagram with the Hamiltonian, and examples of explicit expressions for higher-order charges and examples of the coefficients.
[56] Here, the commutator is denoted as $[A, B] \equiv \frac{1}{2}(AB - BA)$.
[57] M. P. Grabowski and P. Mathieu, Quantum chains with a Catalan tree pattern of conserved charges: The $\Delta = -1$ XXZ model and the isotropic octonionic chain, J. Math. Phys. (N.Y.) **36**, 5340 (1995).
[58] K. Fukai, Proof of completeness of the local conserved quantities in the one-dimensional Hubbard model, arXiv:2309.09354.
[59] B. Pozsgay, Excited state correlations of the finite Heisenberg chain, J. Phys. A **50**, 074006 (2017).
[60] M. Borsi, B. Pozsgay, and L. Pristyák, Current operators in Bethe ansatz and generalized hydrodynamics: An exact quantum-classical correspondence, Phys. Rev. X **10**, 011054 (2020).
[61] B. Pozsgay, Algebraic construction of current operators in integrable spin chains, Phys. Rev. Lett. **125**, 070602 (2020).
[62] M. Borsi, B. Pozsgay, and L. Pristyák, Current operators in integrable models: A review, J. Stat. Mech. (2021) 094001.
[63] K. Fukai, R. Kleinemühl, B. Pozsgay, and E. Vernier, On correlation functions in models related to the Temperley-Lieb algebra, arXiv:2309.07472.
[64] B. Pozsgay, T. Gombor, A. Hutsalyuk, Y. Jiang, L. Pristyák, and E. Vernier, Integrable spin chain with Hilbert space fragmentation and solvable real-time dynamics, Phys. Rev. E **104**, 044106 (2021).
[65] K. Sanada, Y. Miao, and H. Katsura, Quantum many-body scars in spin models with multibody interactions, Phys. Rev. B **108**, 155102 (2023).